J Therm Anal Calorim (2010) 99:501–507
DOI 10.1007/s10973-009-0275-1

Dynamic and controlled rate thermal analysis of halotrichite

Ray L. Frost · Sara J. Palmer · János Kristóf ·
Erzsébet Horváth

Received: 24 May 2009 / Accepted: 26 June 2009 / Published online: 25 July 2009

Abstract Three halotrichites namely halotrichite $Fe^{2+}SO_4{\cdot}Al_2(SO_4)_3{\cdot}22H_2O$, apjohnite $Mn^{2+}SO_4{\cdot}Al_2(SO_4)_3{\cdot}22H_2O$ and dietrichite $ZnSO_4{\cdot}Al_2(SO_4)_3{\cdot}22H_2O$, were analysed by both dynamic, controlled rate thermogravimetric and differential thermogravimetric analysis. Because of the time limitation in the controlled rate experiment of 900 min, two experiments were undertaken (a) from ambient to 430 °C and (b) from 430 to 980 °C. For halotrichite in the dynamic experiment mass losses due to dehydration were observed at 80, 102, 319 and 343 °C. Three higher temperature mass losses occurred at 621, 750 and 805 °C. In the controlled rate thermal analysis experiment two isothermal dehydration steps are observed at 82 and 97 °C followed by a non-isothermal dehydration step at 328 °C. For apjohnite in the dynamic experiment mass losses due to dehydration were observed at 99, 116, 256, 271 and 304 °C. Two higher temperature mass losses occurred at 781 and 922 °C. In the controlled rate thermal analysis experiment three isothermal dehydration steps are observed at 57, 77 and 183 °C followed by a non-isothermal dehydration step at 294 °C. For dietrichite in the dynamic experiment mass losses due to dehydration were observed at 115, 173, 251, 276 and 342 °C. One higher temperature mass loss occurred at 746 °C. In the controlled rate thermal analysis experiment two isothermal dehydration steps are observed at 78 and 102 °C followed by three non-isothermal dehydration steps at 228, 243 and 323 °C. In the CRTA experiment a long isothermal step at 636 °C attributed to de-sulphation is observed.

Keywords Evaporite · Jarosite · Halotrichite · Sulphate · CRTA

R. L. Frost (✉) · S. J. Palmer
Inorganic Materials Research Program, School of Physical and Chemical Sciences, Queensland University of Technology, 2 George Street, GPO Box 2434, Brisbane, QLD 4001, Australia
e-mail: r.frost@qut.edu.au

J. Kristóf
Department of Analytical Chemistry, University of Pannonia, PO Box 158, 8201 Veszprém, Hungary

E. Horváth
Department of Environmental Engineering and Chemical Technology, University of Pannonia, PO Box 158, 8201 Veszprém, Hungary

Introduction

The minerals in the halotrichite group have been known for a long period of time [1–6]. This no doubt is because of their occurrence in environmental systems. These minerals are referred to as the pseudo-alums [7–9], and are often found in the environment as post-mining phases [7–9]. The minerals are monoclinic sulphates of general formula $AB_2(SO_4)_4{\cdot}22H_2O$ where A is Mg^{2+}, Mn^{2+}, Fe^{2+}, Ni^{2+}, Zn^{2+} and/or some combination of these cations and B is Al^{3+}, Cr^{3+} or Fe^{3+} or even a combination of these cations. These minerals have often been referred to as the pseudo-alums. The minerals as with other alums based upon monovalent cations can be readily synthesised in the laboratory. Ions of metals such as manganese, ferrous iron, cobalt, zinc and magnesium will form double sulphates. These sulphates are related to the halotrichites mineral series and often form solid solutions. These alums are not isomorphous with the univalent alums. Typically the end member formulae are $FeSO_4{\cdot}Al_2(SO_4)_3{\cdot}22H_2O$ (halotrichite) or $MgSO_4{\cdot}Al_2(SO_4)_3{\cdot}22H_2O$ (pickeringite), but other M^{2+} cations substitute and solid solutions in the series are extensive. Apjohnite is the manganese equivalent of halotrichite. Wupatkiite is the cobalt analogue, which may have some other divalent metal substitution for the cobalt cation [10]. The minerals are all isomorphous and crystallise in the monoclinic space group *P2₁/c* [11]. In the structure of the pseudo-alums, four crystallographically independent sulphate ions are present [11–15]. One acts as a unidentate ligand to the M^{2+} ion, and the other three are involved in complex hydrogen bond arrays involving coordinated water molecules to both cations and to the lattice water molecules [13].

The thermal decomposition of halotrichite related minerals jarosites has been studied for some considerable time [16–20]. There have been many studies on the Fe(II) and Fe(III) sulphate minerals [21–26]. Interest in such minerals and their thermal stability rests with the possible identification of these minerals and related dehydrated paragenetically related minerals on planets and on Mars. Recently thermogravimetric analysis has been applied to some complex mineral systems [27–29]. It is considered that TG-MS analyses may also be applicable to the jarosite minerals [30–39]. The thermal stability of minerals such as halotrichites which are only formed from solution is important especially for the analysis of minerals on planets such as Mars. Thermal analysis has been used extensively for testing the stability of minerals. To the best of the authors' knowledge no thermoanalytical studies of halotrichites have been undertaken; although differential thermal analysis of some related minerals has been published. In this work we report the thermogravimetric analysis of the thermal decomposition of synthetic halotrichite $FeAl_2(SO_4)_4 \cdot 22H_2O$, apjohnite $MnAl_2(SO_4)_4 \cdot 22H_2O$ and dietrichite $ZnAl_2(SO_4)_4 \cdot 22H_2O$.

Experimental

Synthesis of the halotrichites

Halotrichite

Synthetic halotrichite was prepared by dissolving precisely equimolar masses of iron(II) sulphate and aluminium(III) sulphate in degassed ultra-pure water (18.2 MΩ) the resulting solution was evaporated by a constant stream of nitrogen isolated from atmospheric conditions by an ethylene glycol gas trap. The solution was left to dry under the nitrogen for 5 days. Preliminary studies indicated that the addition of heat to the solution was deleterious to the process of co-precipitation.

Apjohnite and dietrichite

A solution saturated by both aluminium(III) sulphate and manganese(II) sulphate was prepared by adding sufficient quantities of both salts to supersaturate the solution at 353 K, the resulting solution was allowed to cool to room temperature and centrifuged at 3,500 rpm for approximately 30 min. To this solution an equimolar amount of aluminium(III) sulphate and manganese(II) sulphate was added in filter paper bags and left to stand for approximately one week. The resulting precipitate was filtered under vacuum filtration and washed twice with ethanol. Dietrichite was prepared using identical methods as above replacing magnesium(II) sulphate for zink sulphate.

The minerals were analysed by X-ray diffraction for phase purity and by electron probe using energy dispersive techniques for quantitative chemical composition.

Thermal analysis

Dynamic experiment

Thermal decomposition of the samples was carried out in a Derivatograph PC type thermoanalytical equipment (Hungarian Optical Works, Budapest, Hungary) capable of recording the thermogravimetric (TG), derivative thermogravimetric (DTG) and differential thermal analysis (DTA) curves simultaneously. The sample was heated in a ceramic crucible in static air atmosphere at a rate of 5 °C/min.

Controlled rate thermal analysis experiment

Thermal decomposition of the samples was carried out in a Derivatograph PC-type thermoanalytical instrument in an open ceramic crucible in static air atmosphere at a pre-set, constant decomposition rate of 0.10 mg/min. (Below this threshold value the samples were heated under dynamic conditions at a uniform rate of 1 °C/min.) With the quasi-isothermal, quasi-isobaric heating program of the instrument the furnace temperature was regulated precisely to provide a uniform rate of decomposition in the main decomposition stage.

Results and discussion

Dynamic thermal analysis of halotrichite

The dynamic TG pattern together with the DTG and DTA patterns for synthetic halotrichite are shown in Fig. 1. The results of the dynamic experiment are summarised in Table 1. Mass losses observed at 74, 95.5, 102 and 123 °C are assigned to water loss as is confirmed by ion current mass spectrometric results. Mass losses of 1.0, 11.5 and 19.7% are observed. Two further decomposition steps are observed at 319 and 343 °C with mass losses of 2% each. Three higher temperature decomposition steps are

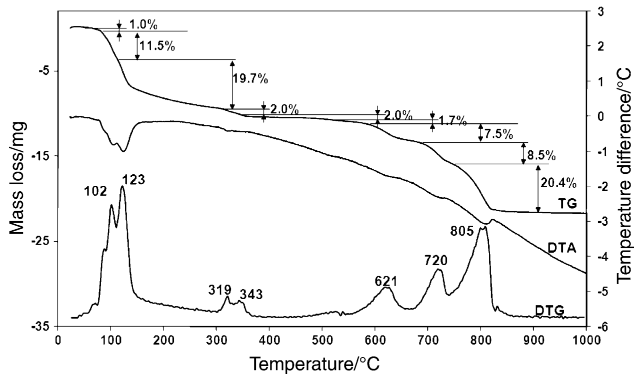

Fig. 1 Dynamic thermal analysis of halotrichite

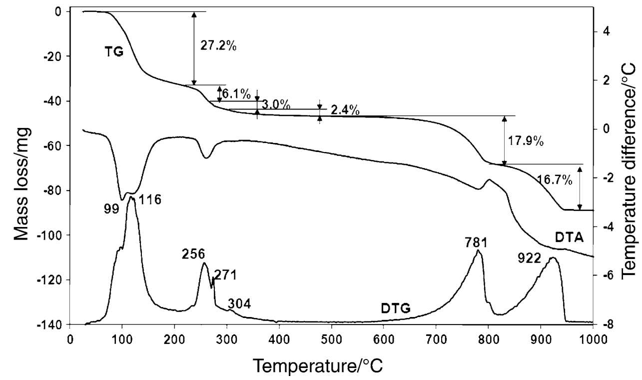

Fig. 2 Dynamic thermal analysis of apjohnite

Table 1 Mass loss and temperature data of halotrichite under dynamic conditions and under CRTA conditions

Decomposition process	Temperature range (°C)	Mass loss	
		mg	%
Dynamic conditions, sample mass: 29.47 mg			
Dehydration	27–74	0.3	1.0
	74–112	3.4	11.5
	112–299	5.8	19.7
	299–333	0.6	2.0
	333–429	0.6	2.0
	429–553	0.5	1.7
Desulphation	553–667	2.2	7.5
	667–739	2.5	8.5
	739–875	6.0	20.4
CRTA conditions, sample mass: 89.53 mg			
Dehydration	27–88	9.9	11.1
	88–124	12.7	14.2
	124–272	7.4	8.3
	272–426	3.6	4.0
CRTA conditions, sample mass: 55.93 mg			
Desulphation	426–542	1.5	2.7
	542–652	6.8	12.2
	652–712	7.5	13.4
	712–795	18.1	32.4
	795–936	0.9	1.6

observed at 621, 720 and 805 °C with mass losses of 7.5, 8.5 and 20.4% making a total mass loss at these temperatures of 36.4%.

The theoretical mass loss of water calculated using the halotrichite formula is 35.68%.

$$\left(Fe^{2+}\right)SO_4 \cdot Al_2(SO_4)_3{\cdot}22H_2O \rightarrow \left(Fe^{2+}\right)SO_4 \cdot Al_2(SO_4)_3{+}22H_2O$$

The measured mass loss for water is 36.2%. Due to the non-standardized storage conditions this difference can be realistic for hydrated minerals. In the three higher

Table 2 Mass loss and temperature data of apjohnite under dynamic conditions and under CRTA conditions

Decomposition process	Temperature range (°C)	Mass loss	
		mg	%
Dynamic conditions, sample mass: 120.64 mg			
Dehydration	54–211	32.8	27.2
	211–265	7.3	6.1
	265–297	3.6	3.0
	297–434	2.9	2.4
Desulphation	537–820	21.6	17.9
	820–965	20.2	16.7
CRTA conditions, sample mass: 194.67 mg			
Dehydration	26–67	10.6	5.4
	67–163	45.0	23.1
	163–263	13.3	6.8
	263–417	5.2	2.7
CRTA conditions, sample mass: 93.21 mg			
Desulphation	417–719	23.4	25.1
	719–789	3.3	3.5
	789–869	25.9	27.8
	869–989	0.5	0.5

temperature steps SO_2 is evolved which was confirmed by mass spectrometry.

The following decomposition is proposed.

$$\left(Fe^{2+}\right)SO_4 \cdot Al_2(SO_4)_3 \rightarrow Al_2O_3 + FeO + 4SO_3 \text{ and } 4SO_3 \rightarrow 4SO_2 + 2O_2$$

Dynamic thermal analysis of apjohnite

The dynamic thermal analysis curves for apjohnite are shown in Fig. 2. The results of the thermal decomposition of apjohnite are shown in Table 2.

A multiple of dehydration steps can be observed up to 400 °C with a total mass loss of 38.7% (the theoretical value is 44.5%):

$$\left(Mn^{2+}\right)SO_4 \cdot Al_2(SO_4)_3{\cdot}22H_2O \rightarrow \left(Mn^{2+}\right)SO_4 \cdot Al_2(SO_4)_3{+}22H_2O$$

Based upon the formula above the total theoretical mass loss is 44.95%.

Some water is apparently retained according to ion current curves to 304 °C. Three additional mass loss steps at 256, 271 and 304 °C are also assigned to water evolution. The total observed mass loss is 38.3% which is somewhat low compared with the theoretical mass loss.

The thermal decomposition steps at 781 and 922 °C are attributed to the decomposition of the sulphate anions in the apjohnite. Such decomposition is confirmed by the ion current curves of SO_2 ($m/Z = 64$) where maxima at 780 and 922 °C are observed. Similar maxima are observed in the ion current curves of oxygen.

The following decomposition is proposed.

$$\left(Mn^{2+}\right)SO_4 \cdot Al_2(SO_4)_3 \rightarrow Al_2O_3 + MnO + 4SO_3 \text{ and } 4SO_3 \rightarrow 4SO_2 + 2O_2$$

The experimental mass loss of 34.6% fits well to the theoretical figure of 36.0%. The overall decomposition is finished by 950 °C.

Dynamic thermal analysis of dietrichite

The dynamic thermal analysis patterns of dietrichite are shown in Fig. 3. A summary of results is reported in Table 3. Thermal decomposition steps are observed at 115, 173, 251, 276, 342 and 746 °C with mass losses of 22.5, 3.6, 3.8, 5.0, 2.8 and 37.0%. The following equation represents the overall dehydration chemistry

$$ZnSO_4 \cdot Al_2(SO_4)_3{\cdot}22H_2O \rightarrow ZnSO_4 \cdot Al_2(SO_4)_3{+}22H_2O$$

The ion current curves support the concept of dehydration at 251, 276 and 342 °C with $m/Z = 17$ and 18 showing maxima at these temperatures. It is interesting to compare the high temperature thermal decomposition of dietrichite.

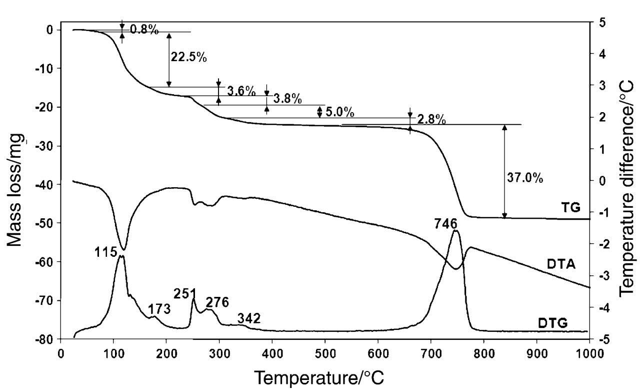

Fig. 3 Dynamic thermal analysis of dietrichite

Table 3 Mass loss and temperature data of dietrichite under dynamic conditions and under CRTA conditions

Decomposition process	Temperature range (°C)	Mass loss	
		mg	%
Dynamic conditions, sample mass: 63.47 mg			
Dehydration	27–70	0.5	0.8
	70–164	14.3	22.5
	164–227	2.3	3.6
	227–264	2.4	3.8
	264–309	3.2	5.0
	309–413	1.8	2.8
Desulphation	589–806	23.5	37.0
CRTA conditions, sample mass: 140.24 mg			
Dehydration	28–88	16.0	11.4
	88–125	19.3	13.8
	125–215	8.1	5.8
	215–236	2.6	1.9
	236–265	3.1	2.2
	265–409	6.0	4.3
	409–497	0.5	0.4
CRTA conditions, sample mass: 84.64 mg			
Desulphation	497–892	51.7	61.1

For halotrichite and apjohnite three mass loss steps are found. The DTG peak of dietrichite is strongly asymmetric and the peak may be curve resolved into three components. The thermal decomposition steps at 746 °C are attributed to the decomposition of the sulphate anions in the dietrichite. Such decomposition is confirmed by the ion current curves of SO_2 ($m/Z = 64$) where maxima at 631, 666 and 692 °C are observed. Similar maxima are observed in the ion current curves of oxygen.

The experimental amount of the crystallization water is 38.5% as compared to the theoretical figure of 44.1%. Dissimilarly to the two former minerals sulphate decomposition is carried out in a single mass loss step at 746 °C:

$$ZnSO_4 \cdot Al_2(SO_4)_3 \rightarrow Al_2O_3 + ZnO + 4SO_3 \text{ and } 4SO_3 \rightarrow 4SO_2 + 2O_2$$

The theoretical mass loss (35.6%) compares well with the observed value of 37.0%.

Controlled rate thermal analysis of halotrichite

The controlled rate thermal analyses of halotrichite are shown in Fig. 4. The results of the Controlled rate thermal analysis (CRTA) are summarised in Table 1. The CRTA experiment is undertaken in two sections (a) up to 400 °C and (b) from 400 to 1,000 °C. The reason for this is that the derivatograph has a time limit of 900 min. For the second experiment, the same sample was placed into the crucible, and with a higher heating rate (2 °C/min) was applied when the pre-set decomposition rate has not been reached (during the first measurement the heating rate was 1 °C/min under this threshold). The higher heating rate is needed to make time and enable the experiment to go in the 900 min. In this way we can resolve the decomposition stage in the higher temperature range.

The CRTA (Fig. 4) shows two quasi-isothermal steps at 82 and 97 °C attributed to dehydration. A non-isothermal higher temperature mass loss is observed at 328 °C and based upon ion current measurements is attributed to dehydration. In between the two experiments the halotrichite sample is cooled to ambient temperatures and adsorbs water from the atmosphere. This accounts for the dehydration step observed at 82 °C in Fig. 4. Three isothermal decomposition steps are observed at 588, 687 and 750 °C and are attributed to the decomposition of sulphate anions.

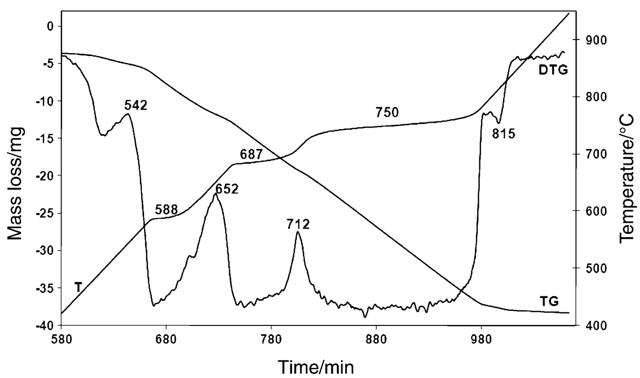

Fig. 4 Controlled rate thermal analysis of halotrichite: ambient to 430 °C, 430–980 °C

Controlled rate thermal analysis of apjohnite

The controlled rate thermal analysis of apjohnite is shown in Fig. 5a (up to 430 °C) and 5b (From 430 to 980 °C). The summary of the CRT analyses are given in Table 2. It is apparent that there are two isothermal decomposition steps at 57 and 77 °C assigned to dehydration. Two higher dehydration mass loss steps are observed at 183 and 294 °C; the first step is a short isothermal step and the second is non-isothermal. Similarly to the dynamic pattern, sulphate decomposition also takes place in two stages under CRTA conditions. In addition to the quasi-isothermal step at 692 °C and the isothermal one at 821 °C, a shoulder peak is observed at 753 °C. This shoulder peak indicates the possible formation of an oxy-sulphate intermediate upon heating.

Controlled rate thermal analysis of dietrichite

The controlled rate thermal analysis of dietrichite is shown in Fig. 6a (up to 430 °C) and 6b (from 430 to 980 °C). The

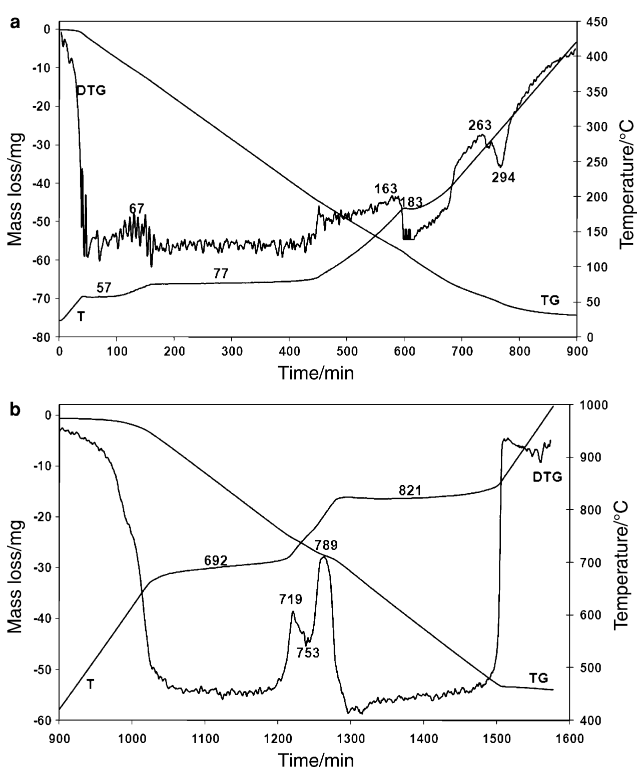

Fig. 5 Controlled rate thermal analysis of apjohnite: **a** ambient to 430 °C, **b** 430–980 °C

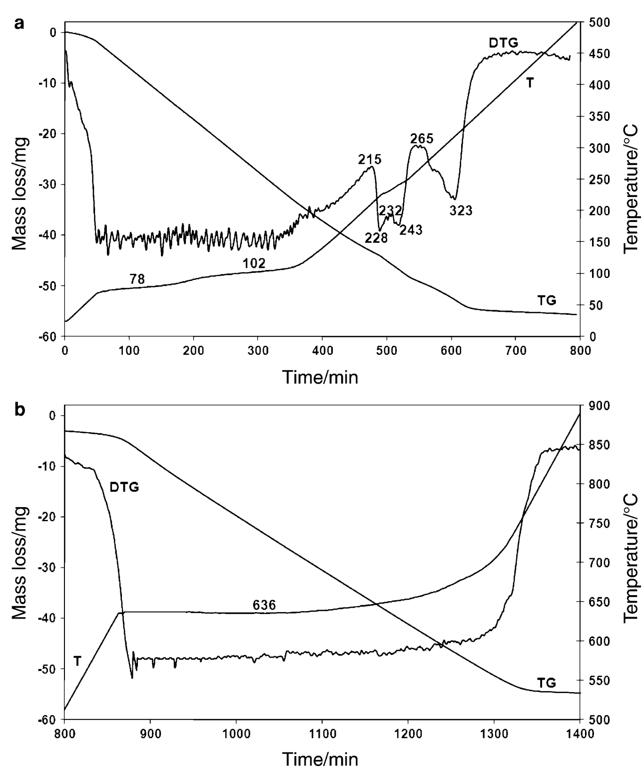

Fig. 6 Controlled rate thermal analysis of dietrichite: **a** ambient to 430 °C, **b** 430–980 °C

thermal analysis patterns (Fig. 6a) show two isothermal steps at 78 and 102 °C which as for the dynamic thermal analysis experiment are attributed to dehydration. Three higher temperature thermal decomposition steps are observed at 228, 243 and 323 °C and are also attributed to dehydration of the dietrichite. (The possible isothermal nature of the higher temperature dehydration steps cannot be proved because the level of decomposition is under the set value of 0.1 mg/min.) Similarly to the dynamic experiment sulphate decomposition is a single step process. The fact that the temperature remained constant at 636 °C for more than 400 min is a proof that the rate-determining step of decomposition is the slow heat transport. Providing time enough for the heat and the mass transport processes to occur, quasi equilibrium decomposition can be reached.

Conclusions

A series of halotrichites also known as pseudo-alums including halotrichite, apjohnite, and dietrichite have been studied by both dynamic thermal and controlled rate thermal analysis. EDX analysis shows the chemical formula of the minerals to be $(Fe^{2+})SO_4{\cdot}Al_2(SO_4)_3{\cdot}22H_2O$, $(Mn^{2+})SO_4{\cdot}Al_2(SO_4)_3{\cdot}22H_2O$, $(Zn)SO_4{\cdot}Al_2(SO_4)_3{\cdot}22H_2O$, respectively. X-ray diffraction showed the minerals to be phase pure except for dietrichite which showed the presence of minor gypsum.

The thermal decomposition of the halotrichite minerals occur through a series of isothermal and non-isothermal steps as is shown by the CRTA experiments. In general a number of dehydration steps are observed up to around 340 °C. These steps are isothermal in the CRTA experiment. The high temperature of the last dehydration steps (343 °C for halotrichite; 304 °C for apjohnite; 342 °C for dietrichite) provides an indication of how strongly hydrogen bonded the water is in the halotrichite structure.

With the use of the CRTA technique the thermal decomposition processes can be standardized. It means that the decomposition temperatures are independent of the experimental conditions offering a solid basis for comparison when concerning the thermal behaviour of a series of minerals is evaluated.

Acknowledgements This research was supported by the Hungarian Scientific Research Fund (OTKA) under grant No. K62175. The financial and infra-structure support of the Queensland University of Technology Inorganic Materials Research Program is gratefully acknowledged.

References

1. Sebor J. Bilinite, a new Bohemian mineral. Prag II: Sbornik Klubu prirodovedeckeho; 1913. 2 pp.
2. Caven RM, Mitchell TC. Equilibrium in systems of the type $Al_2(SO_4)^{3-}M^{II}SO_4$-$H_2O$. I. Aluminium sulfate-copper sulfate-water, and aluminium sulfate-manganous sulfate-water, at 30 Deg. J Chem Soc Trans. 1925;127:527–31.
3. Schurmann HME. Sulfates of magnesium, aluminium and manganese from the Miocene gypsum of Gemsah, east Arabian-Egyptian desert. Neues Jahrb Mineral. 1933;66A:425–32.
4. Baur GS, Sand LB. X-ray powder data for ulexite and halotrichite. Am Mineral. 1957;42:676–8.
5. Velinov I, Aslanyan S, Punev L, Velinova M. Ferrous sulphates, halotrichite, and alunogen from the oxidation zone of the hydrothermally altered volcanic rocks near Krousha village, Sofia District. Izvestiya na Geologicheskiya Institut, Bulgarska Akademiya na Naukite, Seriya Geokhimiya, Mineralogiya i Petrografiya. 1970;19:243–65.
6. Cody RD, Biggs DL. Halotrichite, szomolnokite, and rozenite from Dolliver State Park, Iowa. Can Mineral. 1973;11:958–70.
7. Frost RL, Weier ML, Kloprogge JT, Rull F, Martinez-Frias J. Raman spectroscopy of halotrichite from Jaroso, Spain. Spectrochim Acta. 2005;62A:176–80.
8. Frost RL, Wain DL, Reddy BJ, Martens W, Martinez-Frias J, Rull F. Sulphate efflorescent minerals from the El Jaroso ravine, Sierra Almagrera, Spain—a scanning electron microscopic and infrared spectroscopic study. J Near Infrared Spectrosc. 2006;14:167–78.
9. Xi Y, Zhou Q, Frost RL, He H. Thermal stability of octadecyltrimethylammonium bromide modified montmorillonite organoclay. J Colloid Interface Sci. 2007;311:347–53.
10. Williams SA, Cesbron FP. Wupatkiite from the Cameron uranium district, Arizona, a new member of the halotrichite group. Mineral Mag. 1995;59:553–6.
11. Menchetti S, Sabelli C. The halotrichite group: the crystal structure of apjohnite. Mineral Mag. 1976;40:599–608.
12. Ballirano P, Bellatreccia F, Grubessi O. New crystal-chemical and structural data of dietrichite, ideally $ZnAl_2(SO_4)_4{\cdot}22H_2O$, a member of the halotrichite group. Eur J Mineral. 2003;15:1043–9.
13. Ballirano P. Crystal chemistry of the halotrichite group $XAl_2(SO_4)_4{\cdot}22H_2O$: the X = Fe- Mg-Mn-Zn compositional tetrahedron. Eur J Mineral. 2006;18:463–9.
14. Krstanovic I, Dimitrijevic R, Ilic P. Crystallographic study of halotrichite from Suplja Stena, Avala Mountain. Glasnik Prirodnjackog Muzeja u Beogradu, Serija A: Mineralogija, Geologija, Paleontologija. 1972;27:11–5.
15. Quartieri S, Triscari M, Viani A. Crystal structure of the hydrated sulfate pickeringite [$MgAl_2(SO_4)_4{\cdot}22H_2O$]: X-ray powder diffraction study. Eur J Mineral. 2000;12:1131–8.
16. Nagai S, Yamanouchi N. Potassium ore jarosite. I. Properties of jarosite and leaching test of potassium portion. Nippon Kagaku Kaishi (1921-47). 1949;52:83–6.
17. Kulp JL, Adler HH. Thermal study of jarosite. Am J Sci. 1950;248:475–87.
18. Cocco G. Differential thermal analysis of some sulfate minerals. Period Miner. 1952;21:103–38.
19. Tsvetkov AI, Val'yashikhina EP. Thermal characteristics of minerals of the alunite group. Dokl Akad Nauk SSSR. 1953;89:1079–82.
20. Tsvetkov AI, Val'yashikhina EP. Phase conversions of hydrated iron sulfates (fibroferrite, $Fe(SO_4)(OH){\cdot}4.5H_2O$, and melanterite, $FeSO_4{\cdot}7H_2O$) by heating. Dokl Akad Nauk SSSR. 1953;93:343–6.
21. Swamy MSR, Prasad TP, Sant BR. Thermal analysis of ferrous sulfate heptahydrate in air. II. The oxidation-decomposition path. J Therm Anal Calorim. 1979;16:471–8.
22. Swamy MSR, Prasad TP, Sant BR. Thermal analysis of ferrous sulfate heptahydrate in air. I. Some general remarks and methods. J Therm Anal Calorim. 1979;15:307–14.

23. Bhattacharyya S, Bhattacharyya SN. Heat capacity and enthalpy of the ternary system ferrous sulfate heptahydrate, sulfuric acid, and water. J Chem Eng Data. 1979;24:93–6.
24. Swami MSR, Prasad TP. Thermal analysis of iron(II) sulfate heptahydrate in air. III. Thermal decomposition of intermediate hydrates. J Therm Anal Calorim. 1980;19:297–304.
25. Swamy MSR, Prasad TP. Thermal analysis of iron(II) sulfate heptahydrate in air. V. Thermal decomposition of hydroxy and oxysulfates. J Therm Anal Calorim. 1981;20:107–14.
26. Banerjee AC, Sood S. Thermal analysis of basic ferric sulfate and its formation during oxidation of iron pyrite. In: Thermal analysis: proceedings of the 7th international conference, vol. 1; 1982. p. 769–74.
27. Frost RL, Hales MC, Martens WN. Thermogravimetric analysis of selected group (II) carbonate minerals—implication for the geosequestration of greenhouse gases. J Therm Anal Calorim. 2009;95:999–1005.
28. Palmer SJ, Spratt HJ, Frost RL. Thermal decomposition of hydrotalcites with variable cationic ratios. J Therm Anal Calorim. 2009;95:123–9.
29. Carmody O, Frost R, Xi Y, Kokot S. Selected adsorbent materials for oil-spill cleanup. A thermoanalytical study. J Therm Anal Calorim. 2008;91:809–16.
30. Frost RL, Locke A, Martens WN. Thermogravimetric analysis of wheatleyite $Na_2Cu^{2+}(C_2O_4)_2 \cdot 2H_2O$. J Therm Anal Calorim. 2008;93:993–7.
31. Frost RL, Locke AJ, Hales MC, Martens WN. Thermal stability of synthetic aurichalcite. Implications for making mixed metal oxides for use as catalysts. J Therm Anal Calorim. 2008;94: 203–8.
32. Frost RL, Locke AJ, Martens W. Thermal analysis of beaverite in comparison with plumbojarosite. J Therm Anal Calorim. 2008; 92:887–92.
33. Frost RL, Wain D. A thermogravimetric and infrared emission spectroscopic study of alunite. J Therm Anal Calorim. 2008;91: 267–74.
34. Hales MC, Frost RL. Thermal analysis of smithsonite and hydrozincite. J Therm Anal Calorim. 2008;91:855–60.
35. Palmer SJ, Frost RL, Nguyen T. Thermal decomposition of hydrotalcite with molybdate and vanadate anions in the interlayer. J Therm Anal Calorim. 2008;92:879–86.
36. Vagvoelgyi V, Daniel LM, Pinto C, Kristof J, Frost RL, Horvath E. Dynamic and controlled rate thermal analysis of attapulgite. J Therm Anal Calorim. 2008;92:589–94.
37. Vagvolgyi V, Frost RL, Hales M, Locke A, Kristof J, Horvath E. Controlled rate thermal analysis of hydromagnesite. J Therm Anal Calorim. 2008;92:893–7.
38. Vagvolgyi V, Hales M, Martens W, Kristof J, Horvath E, Frost RL. Dynamic and controlled rate thermal analysis of hydrozincite and smithsonite. J Therm Anal Calorim. 2008;92:911–6.
39. Zhao Y, Frost RL, Vagvolgyi V, Waclawik ER, Kristof J, Horvath E. XRD, TEM and thermal analysis of yttrium doped boehmite nanofibres and nanosheets. J Therm Anal Calorim. 2008;94:219–26.